

# Lambda AntiLambda Production as a Benchmark Channel for PANDA

Marco Destefanis  
Justus Liebig Universität Giessen - Germany  
for the PANDA collaboration

## Abstract

The PANDA [1, 2] experiment which is part of the future FAIR facility at Darmstadt will investigate reactions of antiprotons with hydrogen and nuclear targets. One of the benchmark channel for the simulation and the design of the detector is the  $\Lambda\bar{\Lambda}$  channel, which has been extensively investigated by the PS185 collaboration [3, 4, 5, 6, 7]. This paper will report on first results on GEANT4 simulations including the PANDA detector geometry which have been performed to study the detector acceptance, resolution and background suppression as well as the reconstruction polarization observables.

## 1 Physics and Detector

The PANDA collaboration [1, 2] proposes to build a state-of-the-art universal detector for strong interaction studies at the high-energy storage ring HESR at the international FAIR facility in Darmstadt. The detector is designed to take advantage of the extraordinary physics potential which will be available utilizing high intensity, phase space cooled antiproton beams.

The collaboration is planning to use the antiproton beams, provided by the new FAIR facility, in a momentum range of 1 GeV/c to 15 GeV/c to address fundamental questions on QCD. The fundamental building blocks of QCD are the quarks which interact with each other by exchanging gluons. When the distance between the quarks becomes comparable to the size of the nucleon, the force among them becomes so strong that they cannot be further separated, in contrast to the electromagnetic and gravitational forces which fall off with increasing distance. This unusual behavior is related to the self-interaction of gluons: gluons do not only interact with quarks but also with each other, leading to the formation of gluonic flux tubes connecting the quarks. As a consequence, quarks have never been observed as free particles and are confined within hadrons, complex particles made of 3 quarks (baryons) or a quark-antiquark pair (mesons). Baryons and mesons are the relevant degrees of freedom in our environment. An important consequence of the gluon self-interaction and a strong proof of our understanding of hadronic matter is the prediction of hadronic systems consisting only of gluons (glueballs) or bound systems of quark-antiquark pairs and gluons (hybrids) with both normal and exotic quantum numbers. As illustrated in Fig. 1, the physics program, which can be developed using the HESR storage ring, offers a broad range of investigation that extend from the study of QCD to the test of fundamental symmetries.

In antiproton-proton annihilations, particles with gluonic degrees of freedom as well as particle-antiparticle pairs are copiously produced, allowing spectroscopic studies with unprecedented statistics and precision. The following experiments are foreseen:

- Charmonium ( $c\bar{c}$ ) spectroscopy
- Firm establishment of the QCD-predicted gluonic excitations in the charmonium mass range (3-5GeV/c<sup>2</sup>)

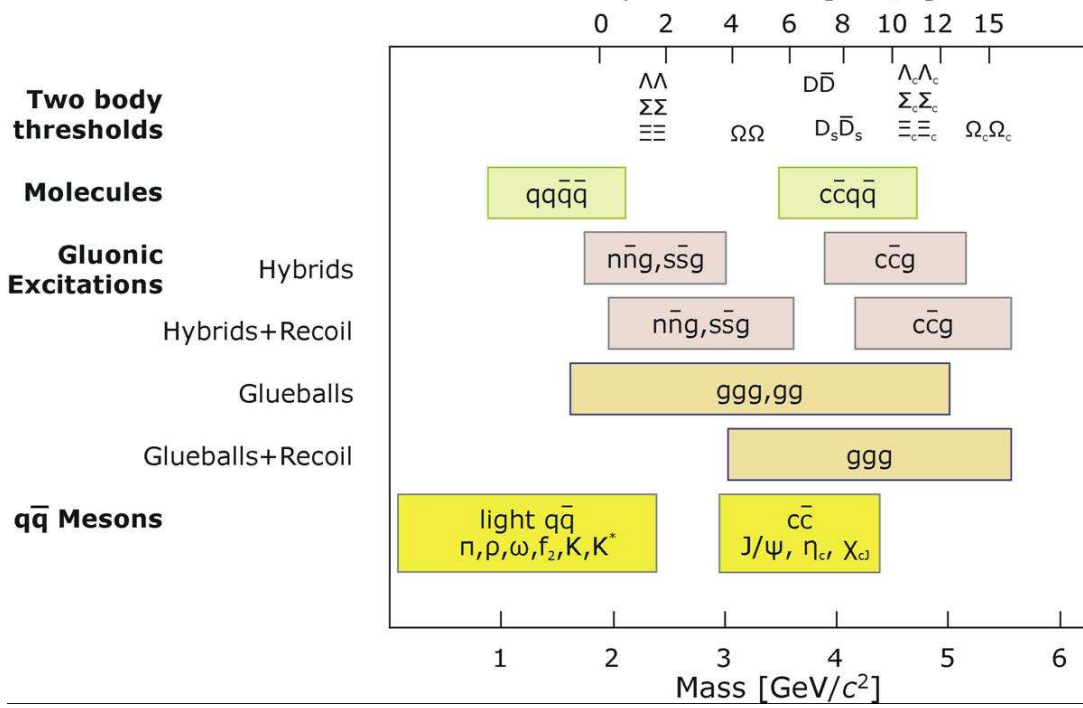


Figure 1: Mass range of hadrons accessible at the HESR with antiproton beams.

- Search for modifications of meson properties in the nuclear medium
- Precision  $\gamma$ -ray spectroscopy of single and double hypernuclei

Further physics opportunities will open up as soon as the HESR facility reaches the full design luminosity:

- Extraction of generalized parton distributions from  $p\bar{p}$  annihilations
- $D$  meson decay spectroscopy
- Search for  $CP$  violation in the charm and strangeness sector ( $D$  meson decays,  $\Lambda\bar{\Lambda}$  system)

The physics program is intensively described in this volume by Tobias Stockmanns.

The physics program, as described, poses significant challenges for the PANDA detector. The tasks are summarized for individual detectors:

- Full angular coverage and good angular resolution for both charged and neutral particles
- Particle identification in a large range of particles ( $\gamma$ -rays,  $e$ ,  $\mu$ , kaons, protons and pions)
- High resolution for a wide range of energies
- High rate compatibility especially for the close-to-target and forward detectors

The detector consists of two spectrometers. A target spectrometer (TS) surrounds the interaction region and a forward spectrometer with a second magnet provides angular coverage for the most forward angles. The basic concept of the target spectrometer is a shell-like arrangement of various detector system surrounding the interaction point inside the field of a large solenoid. The forward spectrometer will cover the gap in detector acceptance in the forward region. The spectrometer apparatus is shown in Fig. 2.

The target spectrometer (TS) is an azimuthally symmetric system of detectors mostly contained inside the superconducting solenoid. This part includes the muon counters on the outside of the

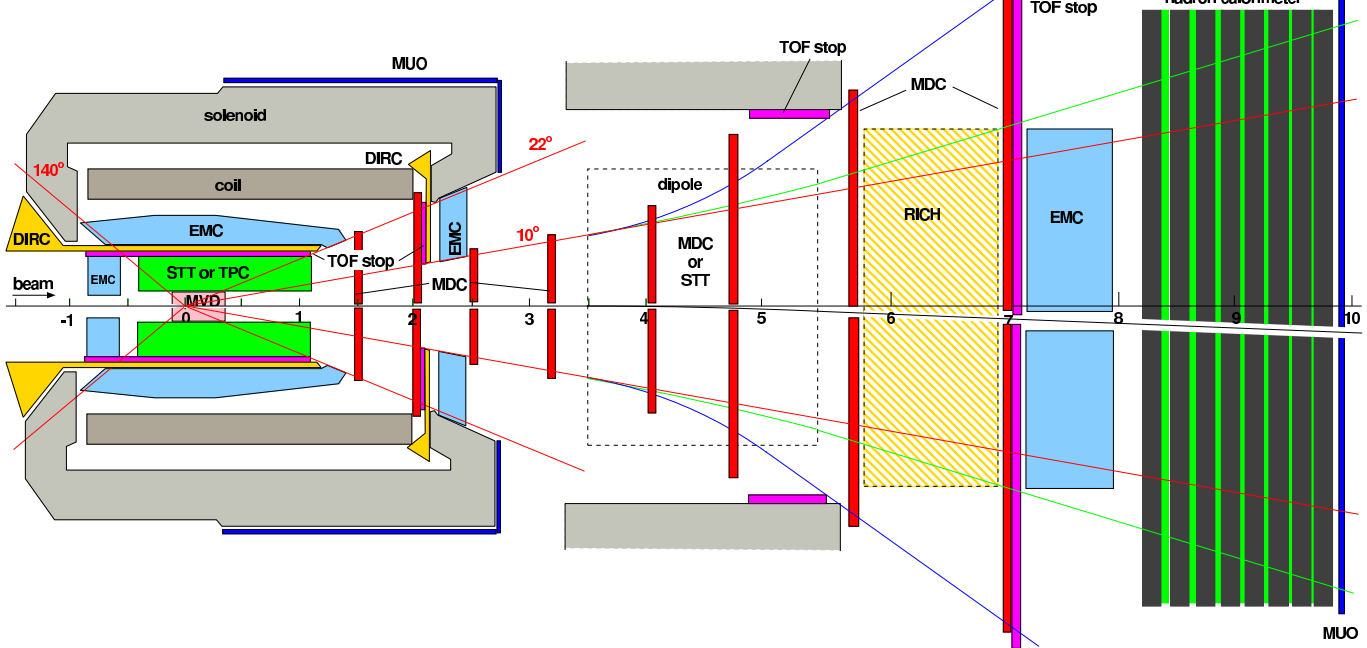


Figure 2: *Setup of the PANDA detector.*

magnet return yoke and the forward end cap which may be situated just behind the magnet. This part of PANDA spectrometer will detect all particles emitted with laboratory angles greater than  $5^\circ$  and  $10^\circ$ , in vertical and horizontal planes respectively, and lower than  $140^\circ$ . No particle detection is foreseen in very backward region of  $170$ - $180$  degrees. Surrounding the interaction volume there will be a silicon micro-vertex detector (MVD). A second tracking detector will consist of 15 double layers of straw tubes (STT). Another possibility is to use time projection chamber (TPC) instead of STT. Particle identification with a ring-imaging Cherenkov (RICH) counter realized by the detection of internally reflected Cherenkov light (DIRC) detector will follow. The forward region will be covered by two sets of mini drift chambers (MDC) and another Cherenkov detector, either aerogel RICH or a flat DIRC. The inner detectors are surrounded by an electromagnetic calorimeter (EMC). It is also planned the use of time-of-flight (TOF) counters for identification of the particles with momenta lower than  $5\text{GeV}/c$ . Outside of the solenoid scintillating bars for muon identification (MUO) will be mounted. For the more forward directed particles tracking and possibly a time of flight start signal will be obtained using the MVD and MDCs.

The current design of the forward spectrometer (FS) includes a 1 m gap dipole and tracking detectors like MDC and straw tube trackers. Photons will be detected by a shashlyk-type calorimeter consisting of lead-scintillators sandwiches (EMC). Particle identification via a ring-imaging Cherenkov (RICH) and time-of-flight counters is previewed. Other neutrals and charged particles with momenta close to the beam momentum will be detected in the hadron calorimeter and muon counters (MUO).

## 2 Motivation

To check deeply such an experimental apparatus and to test the different tracking options the best solution is to take into account a known channel. The channel  $\bar{p}p \rightarrow \Lambda\bar{\Lambda}$  was intensively investigated by the experiment PS185 [3, 4, 5, 6, 7] and can offer a good comparison for our collaboration. In particular, it is important to compare the behaviour of two tracking options: the straw tubes tracker (STT) and the time projection chambers (TPC), shown in Fig. 3 and Fig. 4, respectively.

As main advantages, an STT can offer a robust mechanical stability, an high tracking efficiency due to minimal dead zones of the tubes and especially a high rate capability. The main disadvantage

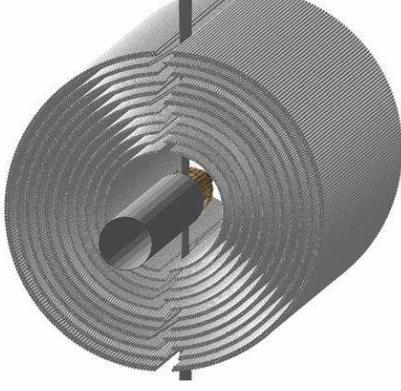


Figure 3: *View of Straw Tube Trackers (STT) with 11 double layers.*

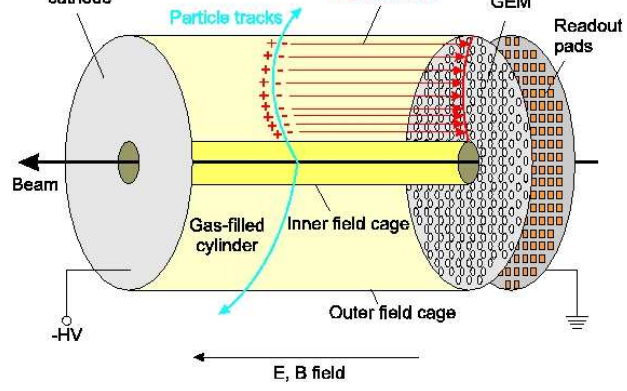


Figure 4: *Schematic view of a GEM based Time Projection Chamber (TPC).*

of STT is the amount of dead material that can cause additional multiple scattering. The TPC tracker can offer high granularity and better particle identification at low momenta in a continuous operation mode. On the other hand a TPC tracker is a slower detector due to the long drift time needed; this can create some problems at high rates, where tracks of several events will overlay and we have to disentangle the tracks of each event from other events.

The results of this comparison will be discussed in the following paragraphs.

With the proposed detector it will be possible to perform the determination of spin observables of the reaction  $\bar{p}p \rightarrow \Lambda\bar{\Lambda}$ . Taking advantage of the self-analyzing power of the parity-violating weak decay  $\Lambda \rightarrow p\pi^-$  ( $\bar{\Lambda} \rightarrow \bar{p}\pi^+$ ), the spin correlation between produced hyperons [8]. This provides a check of the factorization approach and of the hadronization process. When the HESR facility will reach the full design luminosity, it will also be possible to address other physics topics like  $CP$  violation in the strangeness sector.

### 3 Event generation and simulation

The reaction  $\bar{p}p \rightarrow \Lambda\bar{\Lambda}$  was simulated at beam momenta of 4.0,6.0,7.7 GeV/c. Two setup scenarios were investigated: one setup used the straw tube trackers (STT) and the other one used the time projection chambers (TPC). These simulations were done without using the TOF in the target spectrometer and TOF and RICH in the forward spectrometer, presently not implemented, with the consequence that particle identification for certain momentum and angular ranges was not possible. 10000 events were generated. For simplicity and in order to fully cover the detector acceptance, the  $\Lambda$  and the  $\bar{\Lambda}$  particles were generated isotropically in the CM frame, without any decay asymmetry.

The decays  $\Lambda \rightarrow p\pi^-$  and  $\bar{\Lambda} \rightarrow \bar{p}\pi^+$  were studied. Possible background arises from wrong particle ID assumption of  $p-\pi^+$  and  $\bar{p}-\pi^-$  respectively. The PID information was used for proton and pion identification.

At the beam momenta considered,  $\Lambda$  and  $\bar{\Lambda}$  were emitted in the laboratory frame at angles between 0 and 35 degrees for the lowest beam momentum and between 0 and 55 degree for the higher momenta.

### 4 Event Selection

Some cuts on the decay vertex and on the  $\Lambda(\bar{\Lambda})$  invariant mass have been applied for the event selection. Cuts are introduced on the  $\chi^2$  value of the refitted decay vertex ( $\chi^2 < 5.0$ ) and on the  $z$  coordinate of the decay vertex, which is taken between -2.0 mm and 350.0 mm. Both these selections lead to  $\sim 5\%$  event reduction. The angle between  $\Lambda(\bar{\Lambda})$  momentum and the direction of the vector between primary and secondary vertex was also investigated: it was decided to cut angular

the tails of the  $\Lambda(\bar{\Lambda})$  invariant mass distribution accepting a deviation of  $0.003 \text{ GeV}/c^2$  from the  $\Lambda$  mass value of  $1.1157 \text{ GeV}/c^2$ ; this leads to an event reduction of  $\sim 1\%$ .

## 5 Results

The obtained results will reflect the actual status of the PANDA simulation software.

The  $\Lambda$  invariant mass for the beam momentum of  $4.0 \text{ GeV}/c$ , reconstructed from 10000 generated events, is presented in Fig. 5, obtained with the STT setup, and Fig. 6 obtained with the TPC setup, respectively.

Proceeding from the  $\Lambda$  momenta distribution it is clear that the TPC setup allows particle ID even for the slowest tracks. In fact it is possible to reconstruct  $\Lambda$  with a momentum between 1 and  $4 \text{ GeV}/c$  using the STT setup, while the TPC can reconstruct them starting from  $0.5 \text{ GeV}/c$ .

With the STT setup, currently the reconstruction efficiency is only of the order of 25%, which might be due to a loss of low momentum pions in the reconstruction procedure. Clearly, further optimization needs to be done. Using the STT setup, the reconstruction efficiency of  $\bar{\Lambda}$  is lower by 10% as compared to  $\Lambda$  reconstruction. This effect is not present when using the TPC. However, the overall reconstruction efficiency using the TPC reaches only 35%. Mass resolutions of  $0.71 \pm 0.02 \text{ MeV}/c^2$  for STT and  $1.10 \pm 0.02 \text{ MeV}/c^2$  for TPC trackers are obtained, independent of the beam momentum. The tracking options are actually under study to get a better improvement also for the mass resolutions.

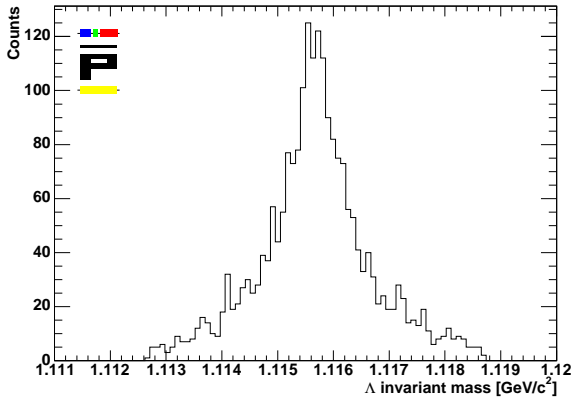


Figure 5:  $\Lambda$  invariant mass spectrum at the beam momentum  $4 \text{ GeV}/c^2$  using STT. Mass resolution:  $0.71 \pm 0.02 \text{ MeV}/c^2$ .

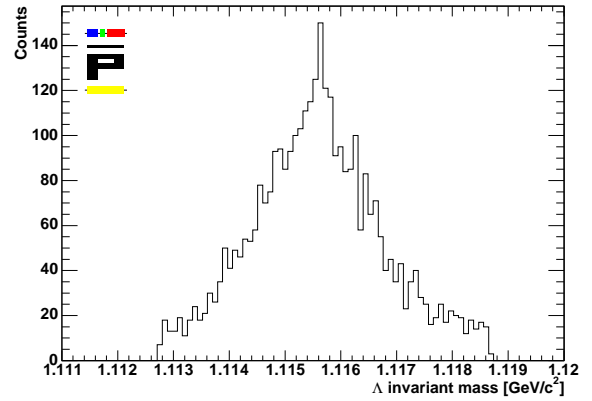


Figure 6:  $\Lambda$  invariant mass spectrum at the beam momentum  $4 \text{ GeV}/c^2$  using TPC. Mass resolution:  $1.10 \pm 0.02 \text{ MeV}/c^2$ .

These peculiarities are also visible in an Armenteros plot. In this plot, the transverse momentum of the decay products in the  $\Lambda$  rest frame is plotted as a function of the asymmetry  $\alpha$ , where  $\alpha = \frac{p_{L+} - p_{L-}}{p_{L+} + p_{L-}}$  and  $p_{L+(-)}$  is the longitudinal momentum of the positive (negative) particle produced in the decay. In Fig. 7 and Fig. 8 the Armenteros plot obtained for both setups are shown.

For the  $\Lambda\bar{\Lambda}$  pair reconstruction with the STT setup it is possible to reach an efficiency of 6%. Using the TPC setup, instead, the reached efficiency is around 25%. The efficiency clearly need to be improved for both the tracking options. The missing momentum, the missing energy and the missing mass were studied for the different beam momenta. In Table 1 the resolutions obtained with a beam momentum of  $4.0 \text{ GeV}/c$  for both setups are shown. It should be noticed that the missing momentum resolution is higher in transverse direction as compared to longitudinal direction. Comparing the STT and the TPC trackers, the STT setup offers a better resolution, but a lower reconstruction efficiency. With both setups, the resolution of the longitudinal missing momentum is worst at the highest beam momenta. Every value of this table should be centred in 0. This indicates the presence of some discrepancies in our simulation or reconstruction routines that needs to be investigated.

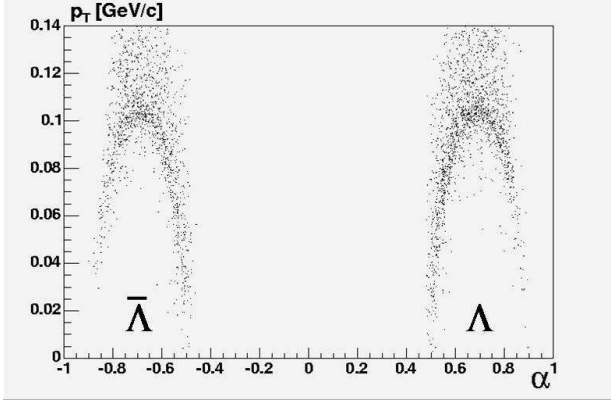


Figure 7: Armenteros plot obtained with STT.

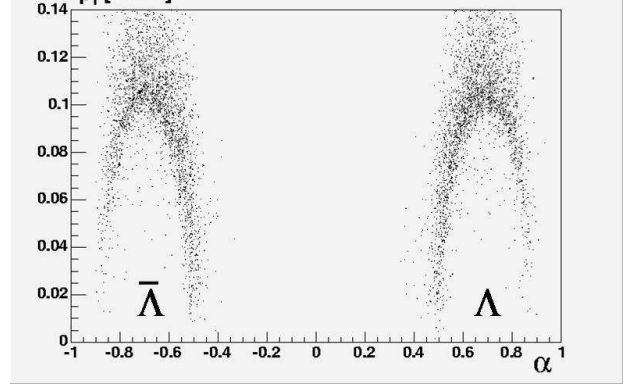


Figure 8: Armenteros plot obtained with TPC.

	STT $mean \pm \sigma$	TPC $mean \pm \sigma$
Missing Energy [MeV]	$19.98 \pm 0.88$	$39.54 \pm 0.88$
Missing Mass [MeV/c <sup>2</sup> ]	$46.43 \pm 2.12$	$80.48 \pm 2.95$
Missing Transverse Momentum [MeV/c]	$9.26 \pm 0.33$	$13.70 \pm 0.20$
Missing Longitudinal Momentum [MeV/c]	$20.28 \pm 0.79$	$35.25 \pm 1.05$

Table 1: Resolution of missing energy, missing mass and missing momentum for a  $\Lambda \bar{\Lambda}$  couple at a beam momentum of 4.0 GeV/c. The mean value  $\pm$  the sigma of the gaussian distribution obtained is presented.

The different beam momenta studied (6.0 and 7.7 GeV/c) give comparable results with the one shown here for a beam momentum of 4 GeV/c.

## 6 Summary

The reconstruction of  $\Lambda \bar{\Lambda}$  pairs is possible with the PANDA spectrometer.

The use of a known channel ( $\Lambda \bar{\Lambda}$ ) gives the possibility to perform the study of the PANDA detector acceptance, resolution and background suppression. In this way, it is also possible to obtain a good comparison between different tracking options, that in the case of my work were Straw Tube Tracker (STT) and Time Projection Chamber (TPC).

These first simulation results pointed out some software problems that need to be fixed in the future. It is also important to add the PID detectors in the target and the forward spectrometer (TOF and RICH) in the simulation geometry to have more improvement. Background studies based on the Dual Parton Model [9] are in progress. Furthermore, we plan to study the decay asymmetry reconstruction of the  $\Lambda$  and the  $\bar{\Lambda}$  particles.

## 7 Acknowledgements

This work was supported in part by DFG, EU, GSI and BMBF.

## References

- [1] PANDA Collaboration, *Letter of Intent for: PANDA, Strong Interaction Studies with Antiproton*, 21/01/2004

[1] *tiproton*, 02/2005

[3] <http://hpfr02.physik.uni-freiburg.de/projects/ps185/ps185.html>

[4] PS185 collaboration, *Letter of Intent PS185*, CERN/PSCC/81-29/159, 1981

[5] PS185 collaboration, *Proposal PS185 'Study of Threshold Production of  $p\bar{p} \rightarrow \text{Antihyperon Hyperon at LEAR}$ '*, CERN/PSCC/81-69/P49, 1981

[6] PS185 collaboration, *Proposal PS185-2 'High precision measurement of  $p\bar{p} \rightarrow \text{Lambdabar Lambda}$  cross sections in the mass region around 2232 MeV/c<sup>2</sup>'*, CERN/SPSLC/92-6/P266, 01/1992

[7] PS185 collaboration, *Proposal PS185-3 'A Measurement of Depolarization and Spin Transfer in  $p\bar{p} \rightarrow \text{Lambdabar Lambda}$ '*, CERN/SPSLC/95-13/P287, 03/1995

[8] S.Belostotski, O.Grebenyuk, *Transverse Polarization of  $\Lambda$  and  $\bar{\Lambda}$  produced inclusively in 99-00 years at HERMES*, 07/2001

[9] A.Capella, U.Sukhatme, C.-I. Tan, J.Tran Thanh Van, *Phys. Rept.* **236**, 225, 2004